A&A 411, L85–L90 (2003)
DOI: 10.1051/0004-6361:20031366

Astronomy & Astrophysics

Neutron-induced nuclear reactions and degradation in germanium detectors

P. Leleux[1], F. Albernhe[2,3], V. Borrel[2,3], B. Cordier[4], R. Coszach[1,⋆], S. Crespin[5], J. M. Denis[1], P. Duhamel[6], P. Frabel[3], W. Galster[1,⋆⋆], J.-S. Graulich[1,⋆⋆⋆], P. Jean[3], B. Kandel[3], J. P. Meulders[1], G. Tauzin[4], J. Vanhorenbeeck[6], G. Vedrenne[3], and P. von Ballmoos[3]

[1] Institut de Physique Nucléaire, Université catholique de Louvain, 1348 Louvain-la-Neuve, Belgium
[2] Institut Universitaire de Technologie, Université Paul Sabatier, 31077 Toulouse, France
[3] Centre d'Étude Spatiale des Rayonnements, Université Paul Sabatier, 31028 Toulouse, France
[4] CEA-Saclay, DSM/DAPNIA/SAP, 91191 Gif-sur-Yvette, France
[5] CEA-Bruyères, DAM/DPTA, 91180 Bruyères-le-Chatel, France
[6] Institut d'Astronomie et d'Astrophysique, Université Libre de Bruxelles, 1050 Bruxelles, Belgium

Received 28 July 2003 / Accepted 4 September 2003

Abstract. We have measured cross sections of neutron-induced nuclear reactions leading to the delayed production of γ-ray lines similar to the ones of astrophysical interest. Conclusions were drawn concerning the expected background in the ^{26}Al 1809 keV line and the ^{7}Be 478 keV line in SPI. The neutron-induced degradation of Ge detectors was studied vs. the neutron energy, the neutron fluence and the detector temperature. Performance recovery of the detectors was studied for different annealing temperatures. Optimum temperature and times for annealing were determined.

Key words. neutron-induced background, neutron damage

1. Introduction

The SPI spectrometer (Vedrenne et al. 2003) onboard ESA's INTEGRAL mission aims at a high resolution spectroscopy of the γ-ray sky in the 20 keV–8 MeV energy range. Gamma-rays are detected in a camera consisting in 19 high-purity Ge detectors cooled down to a temperature of 85–90 K by Stirling cycle cryocoolers. The field-of-view of the camera is defined by an active shield made of BGO crystals. However, the presence of the shield and of other material surrounding the spectrometer has a negative consequence, i.e. an abundant production of neutrons resulting from the interactions of primary cosmic rays. Monte Carlo simulations predict a neutron energy distribution inside the shield displayed in Fig. 1[1]. This paper reports an experimental study of the neutrons impact to the performance of SPI, performed prior to the launch, in two directions:

i) the neutron-induced delayed production of γ-ray lines at the same energy as the ones from astrophysical sources (Sect. 2);
ii) the neutron-induced degradation of the Ge detector's energy resolution and the recovery after annealing (Sect. 3).

2. The background resulting from neutron-induced reactions

2.1. The problem

Neutron interactions in materials located inside the BGO active shield will lead to the delayed production of γ-ray lines. Being delayed, these events will not be vetoed by anticoincidence signals in the active shield. Several neutron-induced γ-ray lines coincide with lines of astrophysical interest:

– The 122 keV and 136 keV lines from the decay of ^{57}Co are a signature of a supernova event. The detection of the 122 keV supernova line from SN1987a) was reported by OSSE (Kurfess et al. 1992). Neutrons interacting with Ni nuclei inside the shield will produce the 122 and

Send offprint requests to: P. Leleux,
e-mail: leleux@fynu.ucl.ac.be
⋆ *Present address*: Office for Scientific, Technical and Cultural Affairs, Brussels, Belgium.
⋆⋆ *Present address*: Tohoku University, Sendai, Japan.
⋆⋆⋆ *Present address*: CERN, Geneva, Switzerland.

[1] Secondary protons are present as well but their abundance is smaller by a few orders of magnitude. Only above an energy of 350 MeV, protons become as abundant as neutrons.

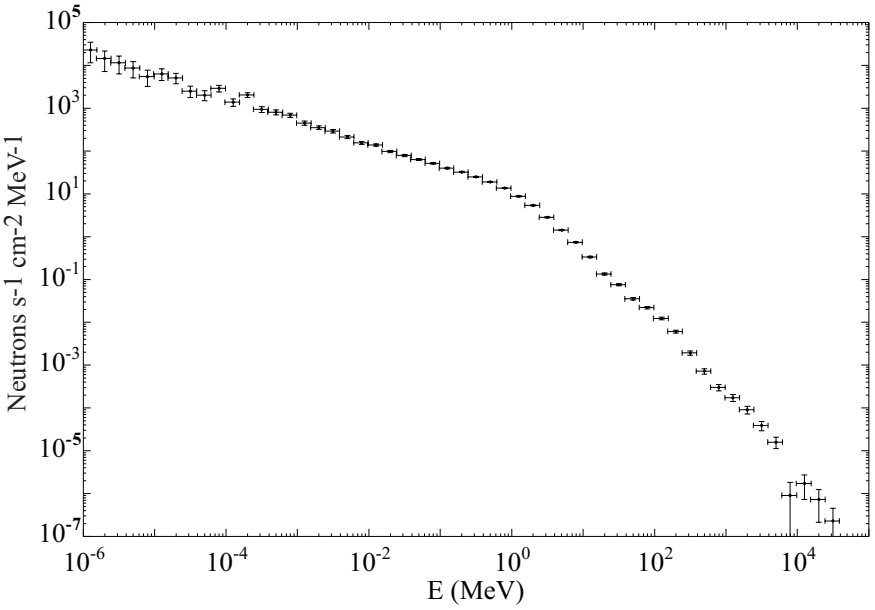

Fig. 1. Neutron energy distribution per sec per cm^2 per MeV inside the shield of SPI.

136 keV lines through the ^{58}Ni(n, 2n)^{57}Ni(β^+)^{57}Co reaction.

- The 478 keV line from ^{7}Be decays is expected from a nova explosion (Hernanz et al. 1996). No positive detection of this line was reported by previous missions. The 478 keV line can result from neutron interaction with Be through the ^{9}Be(n, 3n)^{7}Be reaction.
- The 847 keV line from the radioactive decay of ^{56}Co was detected from SN1987a) (Matz et al. 1988; Teergarden et al. 1989). The ^{56}Fe(n, p)^{56}Mn(β^-)^{56}Fe reaction leads to the emission of the same line.
- The 1157 keV line from ^{44}Ti decay was observed by COMPTEL from the Cas A supernova remnant (Iyudin et al. 1994). This line can be produced by (n, pxn) reactions on all Ti isotopes (x = 2 to 6).
- The emission of ^{60}Fe lines at 1173 keV and 1332 keV, expected from supernovae models (Woosley et al. 1994) has been recently detected for the first time using the RHESSI solar observatory from the general direction of the galactic centre at a level of 15% of the ^{26}Al 1809 keV line flux (Smith 2003). The fact that models predict a ratio of ^{26}Al to ^{60}Fe depending on the mass of the progenitor is of particular interest. Both ^{60}Fe γ-ray lines can be produced by neutron interactions with Copper, by the ^{63}Cu(n, α)^{60}Co reaction (the 1332 keV line only), and the ^{63}Cu(n, 4n)^{60}Cu reaction (both lines are present).
- Finally, the 1809 keV line from ^{26}Al was detected extensively by several missions, including SPI (Diehl et al. 2003) and CGRO, which succeeded to produce a global map of the ^{26}Al activity (Plüschke 2001). In astrophysical sources, this line results in fact from the decay of ^{26}Al to the first excited state of ^{26}Mg, at 1.809 keV above the ground state. Neutron interactions with aluminium through the ^{27}Al(n, 2p)^{26}Na(β^-)^{26}Mg will result in the same line.

  In addition, one should mention that a line at 1811 keV, very close to the ^{26}Al line and in fact within the energy resolution of SPI, can be obtained from the ^{56}Fe(n, p)^{56}Mn reaction reported above.

All the elements quoted above are present inside the BGO shield of SPI. Two of them, Be and Al, are expected to be of importance, as: i) the Ge array is fixed on a Be plate and it is connected to the cryocoolers through a Be cold plate, and ii) each Ge detector is mounted in an Al capsule.

2.2. The solutions

No pessimistic conclusion about the possibility of detecting the above lines from astrophysical sources should be drawn from the previous section. The first point is that most of the above γ-rays belong to a cascade: if one of the γ-rays in the cascade is detected in the shield, the probability for the event to be vetoed is large. In addition, two complementary countermeasures exist:

- The first one (in flight) consists in pointing successively into an astrophysical source emitting a line, and an empty field; this procedure requires the construction of a background model in order to take into account a possible variation of background versus time (or position in orbit).
- The second one (prior to the flight), consists in performing an extensive simulation of neutron interactions with material inside the SPI shield, and deducing the amount of background produced in the lines of interest. Here, a most needed component of the simulation is the cross section for neutron interaction in different material present inside the shield. Although nuclear models have been developed to predict such cross sections, the safest way consists to measure some cross sections over the neutron energy range of interest. The present section reports such measurements.

Table 1. Measured reactions and energy range of each measurement.

Reaction	Energy range (MeV)
^{9}Be(n, 3n)^{7}Be	25–70
^{27}Al(n, 2p)^{26}Na	20–65
^{56}Fe(n, p)^{56}Mn	23–50
^{58}Ni(n, np)^{57}Co	24–69
^{58}Ni(n, 2n)^{57}Ni	24–69
^{63}Cu(n, α)^{60}Co	24–69
^{63}Cu(n, 4n)^{60}Cu	24–69

2.3. The experimental set-up

In the Cyclotron Research Center in Louvain-la-Neuve, a collimated neutron beam was produced by the Li(p, n) reaction induced by a proton beam in the 20–80 MeV energy range (Dupont et al. 1985). The sample was placed at 1 m behind the collimator exit, and irradiated for a period equal to two lifetimes of the isotope of interest. After the irradiation, the sample was removed from the cave and placed in front of a 90% HPGe detector which recorded decay gamma-rays, in a well-shielded area. In a particular measurement, i.e. the ^{27}Al(n, 2p)^{26}Na reaction, the very short lifetime of the final nucleus ^{26}Na (1.09 s) precluded the above procedure. Here a fast mobile arm displaced the sample every two seconds in front of a HPGe detector placed 1 m below the neutron beam and strongly shielded. For each sample, measurements were performed for different proton beam energies, i.e. different neutron energies. The data analysis and the cross section deduction were detailed in a previous publication (Duhamel et al. 1998).

2.4. Results

The measured reactions are summarized in Table 1. Cross sections were fitted over the measured energy range and they were safely extrapolated to higher neutron energies $E \sim$ 100 MeV (Coszach et al. 2000). In two cases, quantitative results regarding the background were deduced from a simulation incorporating a measured cross section and the neutron spectrum of Fig. 1: for the ^{9}Be(n, 3n)^{7}Be reaction, the neutron-induced background in the 478 keV line was found to be 6.4 $\times$ 10^{-3} s^{-1}, while for the ^{27}Al(n, 2p)^{26}Na reaction, the calculated background in the 1809 keV line was 1.0 $\times$ 10^{-2} s^{-1}.

In addition it should be mentioned that all background lines quoted in 2.1, including the 478 keV and the 1809 keV line, have been effectively detected in SPI in orbit (Weidenspointner et al. 2003): in the 470–485 keV region, a complex of lines appear, preventing to isolate the contribution of the 478 keV line. In the 1809 keV line, the background in orbit is 2.9 $\times$ 10^{-2} s^{-1}, about three times the calculated background from the ^{27}Al(n, 2p) reaction; however another reaction ^{27}Al(n, np)^{26}Mg* initiated by neutrons produced outside the shield can contribute to the 1809 keV line. A simulation including measurements of the latter cross section (Brady et al. 1977), allowed to conclude that the sum of the ^{27}Al(n, 2p) and ^{27}Al(n, np) reaction contributions reproduced the observed background.

3. The neutron-induced degradation and recovery of HPGe detectors

3.1. The problem

It has been known experimentally for decades, that Ge detectors are subject to damages when exposed to fast neutrons. Lattice defects acting as charge carrier traps are created in germanium crystals, leading to an increase of the energy resolution of the detector. It is well known also that damages can be repaired by heating the detector and keeping it for some time (normally several days), at a temperature around 100 °C, the so-called annealing process.

In the present geometry of the detectors, i.e. cylindrical, n-type Ge detectors are less sensitive to neutron damage, as holes – the most sensitive carrier type – are collected in the external surface and their average range in the crystal is small. For n-type detectors, significant damage is expected for integrated neutron fluences of about 10^{9} cm^{-2}. Simulations of the neutrons inside the shield of SPI predict this integrated fluence to be obtained in less than two years, i.e. the nominal lifetime of the instrument. It was thus decided from the early design of SPI, to embark onboard a heating system able to anneal the detectors in order to repair the damage.

The study reported in the present section aimed at answering several questions regarding the damage and the recovery.

3.2. Experimental procedure

– Three different neutron beams were used: two monoenergetic beams of 5 MeV and 16 MeV, produced in Bruyères-le-Chatel (France) by the D(d,n)^{3}He and the T(d,n)^{4}He reaction, respectively and a continuous beam from 6 to 70 MeV with a 27 MeV mean energy produced in Louvain-la-Neuve (Belgium) by the p + ^{9}Be interaction at 65 MeV energy. The latter beam simulates quite well the neutron energy distribution to which detectors will be exposed in orbit. In addition, neutrons below 70 MeV represent 96% of the total neutron flux in orbit.
– Flight model detectors were irradiated with different neutron fluences ranging from 3.6 $\times$ 10^{8} cm^{-2} to 1.6$\times$$10^{9}$ cm^{-2} in different neutron beams. Detectors were irradiated with high-voltage (HV) ON, at liquid nitrogen temperature (77 K).
– The parameters used to estimate the damage were the ratio of the Full-Width-at-Tenth-of-Maximum (FWTM) to the Full-Width-at-Half-Maximum (FWHM), and the relative increase of the FWTM or the FWHM. The ^{60}Co peak at 1332 keV was selected for that purpose. Figure 2 shows this peak before and after a neutron irradiation: incomplete charge collection leads to a tail to the left of the peak.
– Annealings were performed with the detector capsule being pumped down to a pressure of a few 10^{-6} Torr.

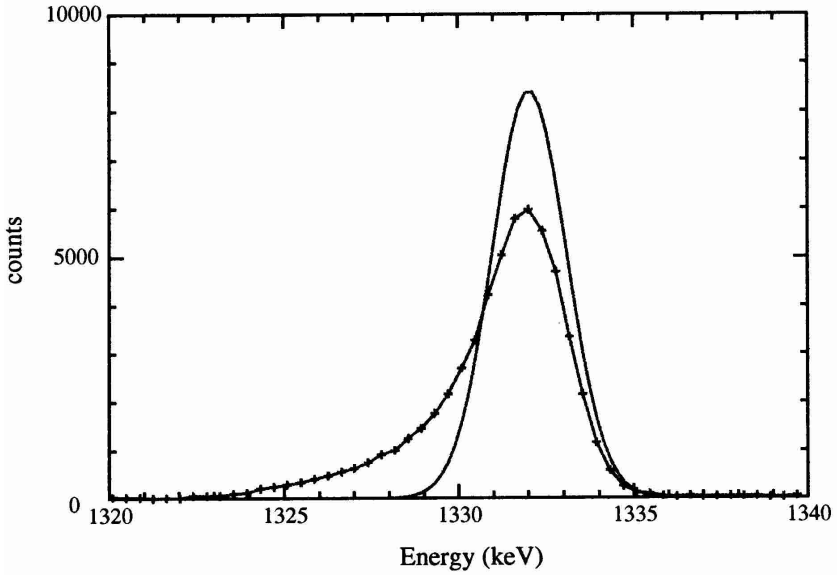

Fig. 2. The 1332 keV ^{60}Co peak after neutron irradiation (dotted line), compared with an ideal (Gaussian) detector (solid line). The total number of counts in both spectra is the same. After irradiation, the number of counts at maximum is reduced by 30% and the width of the region encompassing 10–90% of the peak integral is increased from 3.45 keV (Gaussian detector) to 5.24 keV (degraded detector).

3.3. Results

3.3.1. Damage versus neutron fluence and neutron energy

The dependency of damages versus neutron energy and fluence is illustred in Fig. 3.

For 16 MeV neutrons, the degradation versus the neutron fluence was measured up to 5×10^9 n/cm^2. No saturation of the damage is appearing for either measured variable, i.e. the relative increase of the FWHM and the FWTM. In the same figure, the degradation versus the neutron energy was also plotted; it shows the extreme sensitivity of both variables to the neutron energy. In particular, the relative increase of the FWTM is rising very quickly for high-energy neutrons, prohibiting to submit the detector to fluences larger than 6×10^8 n/cm^2. Let us recall that the energy distribution of the 6–70 MeV neutrons is close to the one expected in orbit. From the data of Fig. 3, an annealing in orbit appears mandatory after a fluence of about 6×10^8 n/cm^2 at most.

3.3.2. Damage versus detector temperature

Although unlikely, a failure of a cryocooler in orbit cannot be excluded. Such a failure would cause an increase of the Ge detectors temperature. Two detectors were irradiated in the continuous 6–70 MeV neutron beam while they were at different temperatures, i.e. 91 K and 110 K. The data are displayed in Fig. 4. Clearly the damage in the "hot" detector was more important and it increased faster at lower fluences. When cooled down to a lower temperature (92 K) after the irradiation, this detector showed a partial recovery of the energy resolution. The conclusions of this section are twofold: i) a detector in orbit should be operated at a temperature as low as possible in order to delay the radiation damage and ii) a detector submitted to a temporary stay at high temperature will not recover its original resolution when replaced to a lower temperature.

3.3.3. Annealings

The strategy was the following: a detector was first submitted to a neutron fluence of 3.6×10^8 n/cm^2 in the 6–70 MeV energy range. One day after the irradiation, the detector activity had decreased enough for a resolution measurement to be done, and the initial degradation to be estimated. Then the detector was warmed up to the annealing temperature. The annealing was interrupted after each period of about 24 h in order to measure the detector energy resolution with a ^{60}Co source, and then started again; this sequence was repeated several times (Albernhe et al. 2002). The parameter of interest was the annealing temperature: when these measurements were performed, the temperature of the annealings in orbit was not yet decided and it was interesting to measure beforehand the loss of observation time caused by an annealing. Annealings were performed at three different temperatures, 94 °C, 100 °C and 105 °C. Results are displayed in Fig. 5. The parameter measured here is the ratio of the FWTM to the FWHM of the 1332 keV ^{60}Co peak, which should be equal to 1.82 for a Gaussian peak. The neutron irradiation caused an increase of this parameter by 40–60% (zero time, before annealing). Data indicate that an annealing at 94 °C does not provide with a full recovery after 8 days, the FWTM/FWHM ratio being then 10% larger than the Gaussian value ; in fact an additional period of a few days at 100 °C (not depicted in Fig. 5) was requested in order to complete the return to the original resolution. On the other hand, the annealing at 105 °C yielded a fast recovery. As a consequence, the design of the SPI camera and its surroundings were adapted to withstand this last-mentioned temperature.

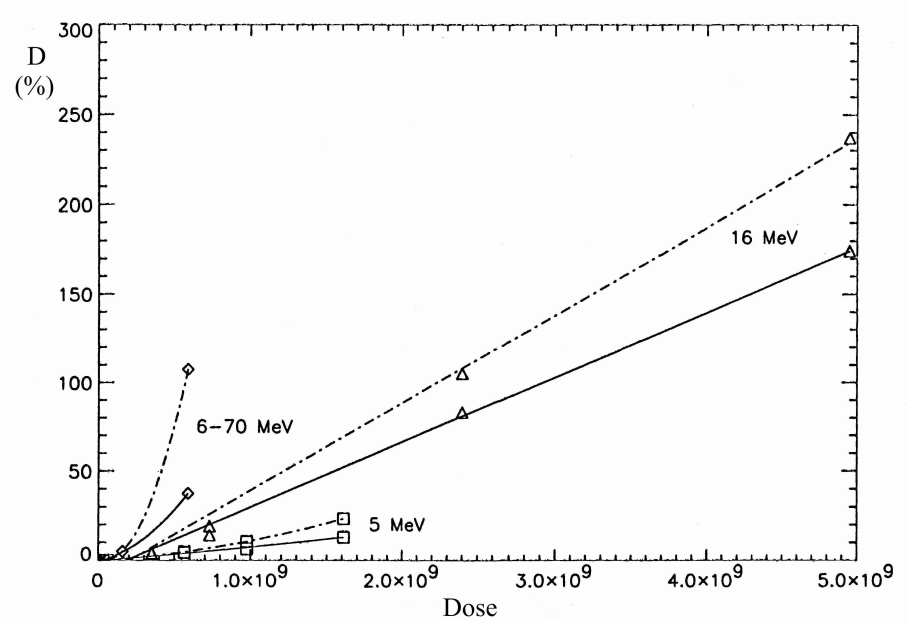

Fig. 3. Degradation of a Ge detector (D, in %) vs. the neutron fluence (in n/cm^2), for different neutron beams (5 MeV, 16 MeV, 6–70 MeV). Two parameters are measuring the degradation: the relative increase of the FWHM (solid line) and the relative increase of the FWTM (dot-dashed line).

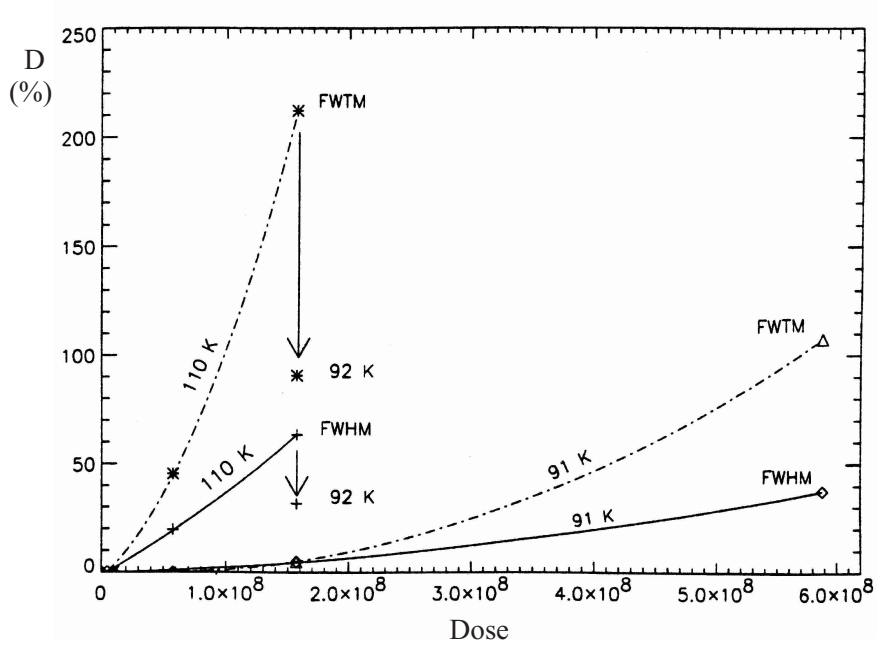

Fig. 4. Degradation (D, in %) vs. the neutron fluence (in n/cm^2), for two detectors irradiated at 91 K and 110 K. The degradation was measured by the relative increase of the FWHM (solid line) or the relative increase of the FWTM (dot-dashed line). After the irradiations, the 110 K detector was returned to 92 K: vertical arrows indicate the recovery obtained.

4. Conclusions

The impact of neutrons on the performance of the SPI Ge detectors was studied experimentally in two fields, the neutron-induced background in the gamma-ray lines, and the neutron-induced degradation and recovery of the detectors. In the first domain, cross section measurements aiming at a better accuracy of the simulations were performed. In the second case, the degradation was measured versus the neutron fluence and the detector temperature, and the recovery was obtained for different annealing temperatures.

It should be noted that since the launch of INTEGRAL, a first annealing of the SPI detectors was performed, on Feb. 6, 2003, i.e. after 110 days in orbit. At that time, the FWHM of the detectors had increased on average by 15 % w.r.t. the original values. The annealing temperature of 105.7° was maintained for 37 h. A complete recovery of the resolution was found after annealing, as expected from our data in Fig. 5.

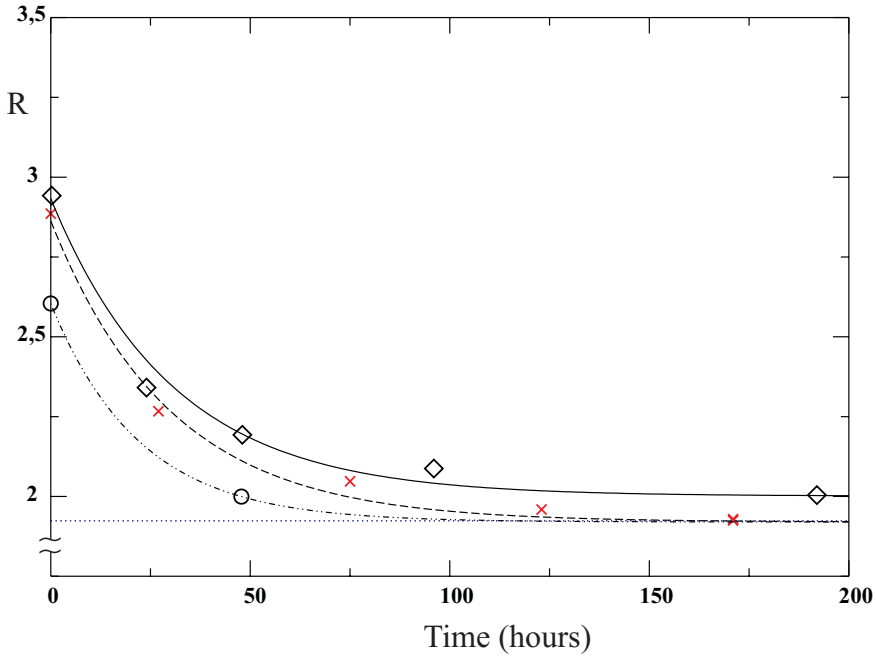

Fig. 5. Recovery (R) of a detector vs. the annealing time. The parameter used to quantify the recovery is the FWTM/FWHM ratio, which is equal to 1.82 for a perfect detector (horizontal dotted line). Annealings were performed at three different temperatures: 94 °C (diamonds fitted with the solid line); 100 °C (crosses fitted with the dashed line), and 105 °C (open dots fitted with the dot-dashed line).

Acknowledgements. This work was granted by a PRODEX budget from the Office for Scientific, Technical and Cultural Affairs, Brussels. Jürgen Knödlseder is acknowledged for useful comments. P.L. is a Research Director of the National Fund for Scientific Research, Brussels.

References

Albernhe, F., Borrel, V., Frabel, P., et al. 2002, Nucl. Instr. Meth. Phys. Res., A492, 91
Brady, F. P., Shepard, J. R., King, N. S. P., et al. 1977, Nucl. Phys., A288, 269
Coszach, R., Leleux, P., Galster, W., et al. 2000, Phys. Rev., C61, 064615
Diehl, R., Knödlseder, J., Lichti, G. G., et al. 2003, A&A, 411, L451
Duhamel, P., Galster, W., Graulich, J.-S., et al. 1998, Nucl. Instr. Meth. Phys. Res., A404, 143
Dupont, C., Leleux, P., Lipnik, P., et al. 1985, Nucl. Phys, A445, 13
Hernanz, M., Jordi, J., Coc, A., et al. 1996, ApJ, 465, L27
Iyudin, A. F., Diehl, R., Bloemen, H., et al. 1994, A&A, 284, L1
Kurfess, J. D., Johnson, W. N., Kinzer, R. L., et al. 1992, ApJ, 399, L137
Matz, S., Share, G. H., Leising, M. D., et al. 1988, Nature, 331, 416
Plüschke, S. 2001, Ph.D. Thesis, Technische Universität München, MPE-Report 276
Smith, D. 2003, in Astronomy with Radioactivities IV, in press
Teegarden, B. J., Barthelmy, S. D., Gehrels, N., et al. 1989, Nature, 339, 122
Vedrenne, G., Roques, J.-P., Schönfelder, V. et al. 2003, A&A, 411, L63
Weidenspointner, G., Kiener, J., Gros, M., et al 2003, A&A, 411, L113
Woosley, S. E., & Weaver, T. A. 1994, ApJ., 423, 371